DOT/FAA/CT-94/57

FAA Technical Center
Atlantic City International Airport,
N.J. 08405

Reduction of Incremental Load Factor Acceleration Data to Gust Statistics

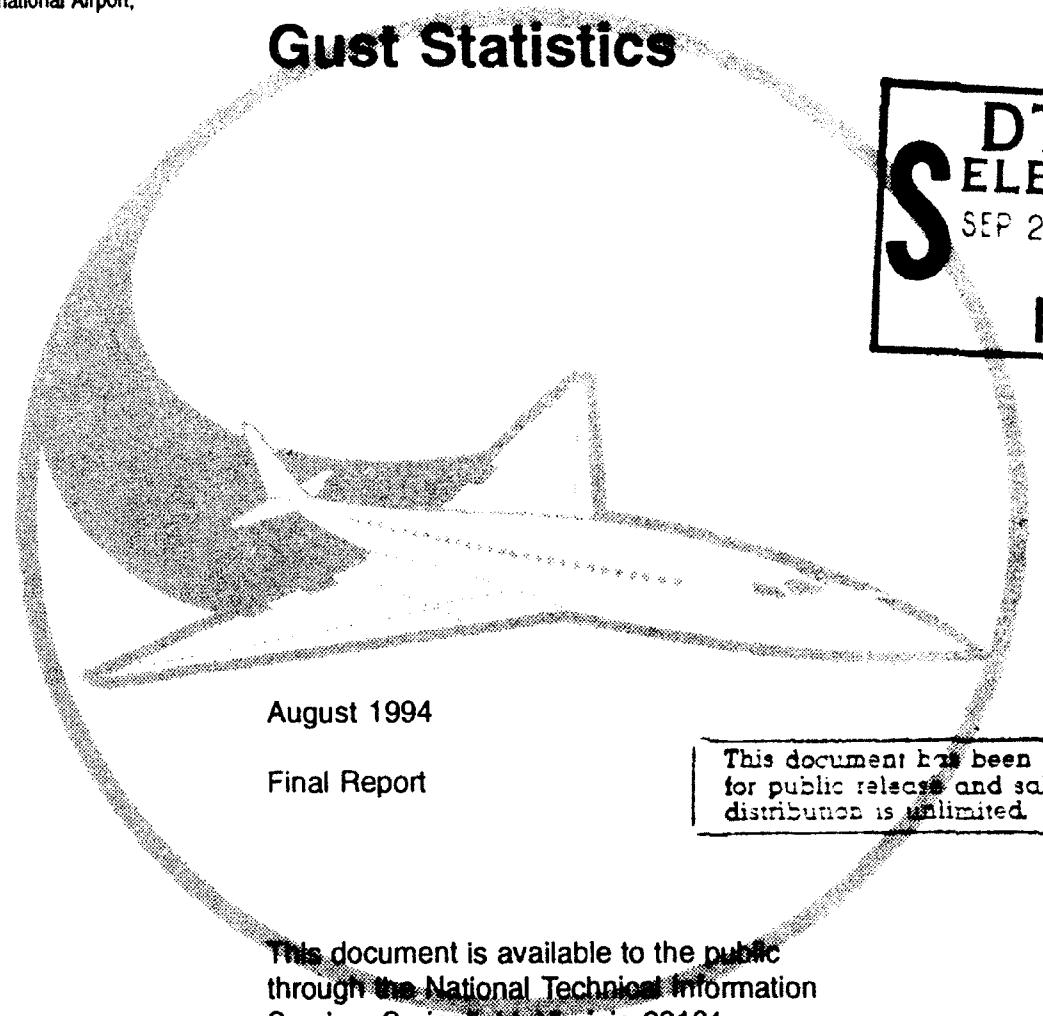

August 1994

Final Report

U.S. Department of Transportation
Federal Aviation Administration

NOTICE

This document is disseminated under the sponsorship of the U. S. Department of Transportation in the interest of information exchange. The United States Government assumes no liability for the contents or use thereof.

The United States Government does not endorse products or manufacturers. Trade or manufacturers' names appear herein solely because they are considered essential to the objective of this report.

Technical Report Documentation Page

1. Report No.	2. Government Accession No	3. Recipient's Catalog No.
DOT/FAA/CT-94/57		

4. Title and Subtitle	5. Report Date
Reduction of Incremental Load Factor Acceleration Data to Gust Statistics	August 1994
	6. Performing Organization Code

7. Author(s)	8. Performing Organization Report No.
J. B. de Jonge	NLR CR 92003L

9. Performing Organization Name and Address	10. Work Unit No. (TRAIS)
National Aerospace Laboratory P.O. Box 90502 1006 BM Amsterdam The Netherlands	MNS-193, RPI 167
	11. Contract or Grant No. OV/RLD-182

12. Sponsoring Agency Name and Address	13. Type of Report and Period Covered
U.S. Department of Transportation Federal Aviation Administration Technical Center Atlantic City International Airport, NJ 08405	Final Report
	14. Sponsoring Agency Code ACD-220

15. Supplementary Notes

This work was performed under a memorandum of cooperation between the Federal Aviation Administration and the Netherlands Civil Aviation Department. As a part of this effort, the National Aerospace Laboratory was contacted to participate in this research effort. The FAA technical manager: Thomas DeFiore, ACD-220.

16. Abstract

This report defines a general procedure for the reduction of center of gravity vertical acceleration data towards gust statistics. The specific aspects treated included: (1) separation of accelerations due to gusts and maneuvers, (2) definition of peaks and valleys, (3) reduction of accelerations to gust velocities using either a discrete- or a continuous-gust concept. The possibility of reevaluating and reducing existing European load sources into a format compatible with the defined general reduction procedure is investigated.

17. Key Words	18. Distribution Statement
Flight Loads, Maneuvers, Aircraft Response, Discrete Gusts, Continuous Gusts	This document is available to the public through the National Technical Information Service, Springfield, Virginia 22161

19. Security Classif. (of this report)	20. Security Classif. (of this page)	21. No. of Pages	22. Price
Unclassified	Unclassified	32	

TABLE OF CONTENTS

LIST OF FIGURES

LIST OF SYMBOLS

$\bar{A}$	- PSD gust response, $\sigma\Delta n/\sigma_w$, or $\Delta n/U\sigma$	(s/m)
$\bar{C}$	- Discrete gust response, $\Delta n/U_{de}$	(s/m)
C_{L_α}	- Aircraft lift curve slope	(rad^{-1})
$\bar{c}$	- wing chord	(m)
g	- gravity constant	(9.81 m/s^2)
m	- aircraft mass	(kg)
n_z	- vertical load factor	
Δn_z	- incremental load factor = n_z-1	
S	- wing area	(m^2)
V	- aircraft speed	(m/s)
V_E	- equivalent speed, $V\sqrt{\frac{\rho}{\rho_o}}$	(m/s)
h	- altitude	(m)
L	- turbulence scale	(= 762 m)

N(0),	number of zero crossings per km	
B_1B_2,	gust frequency parameters in "discrete" gust description	(km^{-1})
a_1, a_2	gust intensity parameters in discrete gust description	(m/s)
P_1, P_2	gust frequency parameters in PSD-gust description	
b_1, b_2	gust intensity parameters in PSD-gust description	(m/s)

subscript 0: reference to sea level
1: reference to "non-storm" conditions
2: reference to "storm" conditions

F(μg)	= "discrete" gust alleviation factor	
F(PSD)	= "continuous" gust alleviation factor	
U_{de}	= derived gust velocity, discrete gust model	(m/s equivalent speed)
U_σ	= derived gust velocity, continuous gust model	(m/s equivalent speed)
ρ	air density	(kg/m^3)
α	angle of incidence	(rad)
ϕ	bank angle	(rad)

μ_g - mass parameter, - $\frac{2m}{\rho\bar{c}SC_{L_\alpha}}$

EXECUTIVE SUMMARY

This report defines a general procedure for the reduction of center of gravity vertical acceleration data towards gust statistics. The specific aspects treated include: (1) Separation of accelerations due to gusts and maneuvers. (2) Definition of peaks and valleys. (3) Reduction of accelerations to "gust velocities", using either a discrete or a continuous gust concept. The possibility of reevaluating and reducing existing European Load Data sources into a format compatible with the defined general reduction procedure is investigated.

1. INTRODUCTION.

As part of the research program on aging aircraft, the Federal Aviation Administration (FAA) has started an ambitious program on flight loads. A large number of transport aircraft will be equipped with multiparameter recording devices to collect statistical data on aircraft loads in actual service conditions.

The Netherlands Civil Aviation Department (RLD) and the FAA have signed a memorandum of cooperation in the area of aircraft structural integrity, with specific reference to aging aircraft. As part of this cooperation, the National Aerospace Laboratory (NLR) was contracted to participate in the flight loads program. One of the tasks specified is the acquisition and review of European sources of flight load data and the reduction of these data into gust statistics using a unified reduction procedure. This data reduction procedure should be compatible with the analysis format to be applied to the data acquired in the current FAA flight load recording program. This report describes the procedures proposed for the reduction of center of gravity (vertical acceleration data[1]) gust statistics.

In the development of these procedures, it will be generally assumed that a continuously recorded acceleration time trace is available for analysis, accompanied by additional data on speed, altitude, weight, aircraft configuration, etc. Specific aspects treated successively include:

a. The separation of accelerations due to gusts and maneuvers.

b. The definition of peaks and valleys in the acceleration trace.

c. The reduction of Δn peaks/valleys to gust velocities.

It will be proposed to simultaneously apply two reduction techniques: one based on a discrete gust model using the so-called Pratt formula and the other based on a continuous PSD-gust model.

Much of existing old load data bases for the most part are available only in a very reduced format. Methods to reevaluate this data will be discussed in section 6, with specific reference to the acquired European data sources, namely NLR Boeing 747 ACMS data, ONERA-high load data, and RAE fatiguemeter data. The report concludes with a summary of proposed data reduction and analysis procedures.

2. SEPARATION OF ACCELERATIONS DUE TO MANEUVERS AND GUSTS.

The incremental vertical acceleration at the center of gravity (c.g.) may be due to either maneuvers or gusts. When deriving gust statistics from acceleration traces it seems logical to remove the maneuver-induced acceleration as accurately as possible from the acceleration history and consider the remaining trace as purely gust-induced acceleration. In the past, for example, in reducing the NACA/NASA VGH recordings, this separation of maneuvers and gusts was done manually by viewing the (analog) record traces. Recently however, separation was

---

[1] Appendix A gives a definition of "c.g. vertical acceleration" as meant in the present report.

obtained by passing the acceleration signal through a variety of filters (reference 1).

Figure 1, reproduced from reference 1, provides an example of the type of result obtained with this procedure, illustrating the possible ways in which accelerations due to maneuvers and gusts may occur, either separately or superimposed. The upper figure shows the unfiltered trace. The second figure shows the acceleration signal after filtering by a low-pass filter; the acceleration trace left is thought to be due to maneuvering. The lower figure shows the high-pass filtered signal, showing accelerations due to gusts. Considering this figure in some more detail, it turns out that the complete separation of maneuvers and gusts may be less desirable than originally perceived.

On the top of upper figure, five typical events are indicated, namely it

1. Shows a typical acceleration trace due to a turning maneuver.

   - The induced incremental acceleration is always positive, and has a relatively long duration (from several seconds up to a few minutes)

   - The Typical magnitude is in the order of 0.15 g (30° bank turn).

2. Shows the same type of turning maneuver with gust loads superimposed. Typically, one may think of turbulence encountered while holding at relatively low altitude.

3. Shows a relatively short duration acceleration peak, probably due to a pitching maneuver. Positive pitching maneuvers occur typically at takeoff, during rotation, and before landing in flare. The magnitude is usually limited to the order of 0.10g. Downward pitching maneuvers occur at the transition from climb to cruise and from cruise to descent. The magnitudes of these pitch-down maneuvers are equally small or probably smaller than those of the pitch-up maneuvers.

4. Shows a pure-gust encounter. The acceleration trace has a highly irregular character with relatively high-frequency content.

5. Shows a trace where maneuver loads are superimposed on the gust loads. Note that the maneuver loads are both upward and downward and of a rather irregular nature. Obviously these maneuvers are a result of the turbulence encounter: the pilot applies his controls to counteract the effect of the turbulence. The latter type of maneuvering cannot be considered independently; it is due to turbulence and should be considered as part of the aircraft response to gust input. Hence, one may decide that it is actually undesirable to filter out this low-frequency part of gust-induced loading. It should be noted that this gust-induced maneuvering is largely in pitch; corrective turns in turbulence remain very limited indeed.

The majority of maneuver-induced loads associated with turning maneuvers can be estimated by using bank angle information. If the bank angle is recorded, the acceleration trace may be corrected for turning maneuvers by subtracting a $\Delta n_{corr} = (1/\cos\phi - 1)$, where ϕ is the bank angle (reference 2).
This procedure will take care of the type 1 and type 2 events from figure 1. As explained before, the majority of pitching maneuvers of type 3 will occur at specific points in the flight profile: specifically, the maneuvers at rotation and flare can easily be traced and removed from the acceleration trace using a

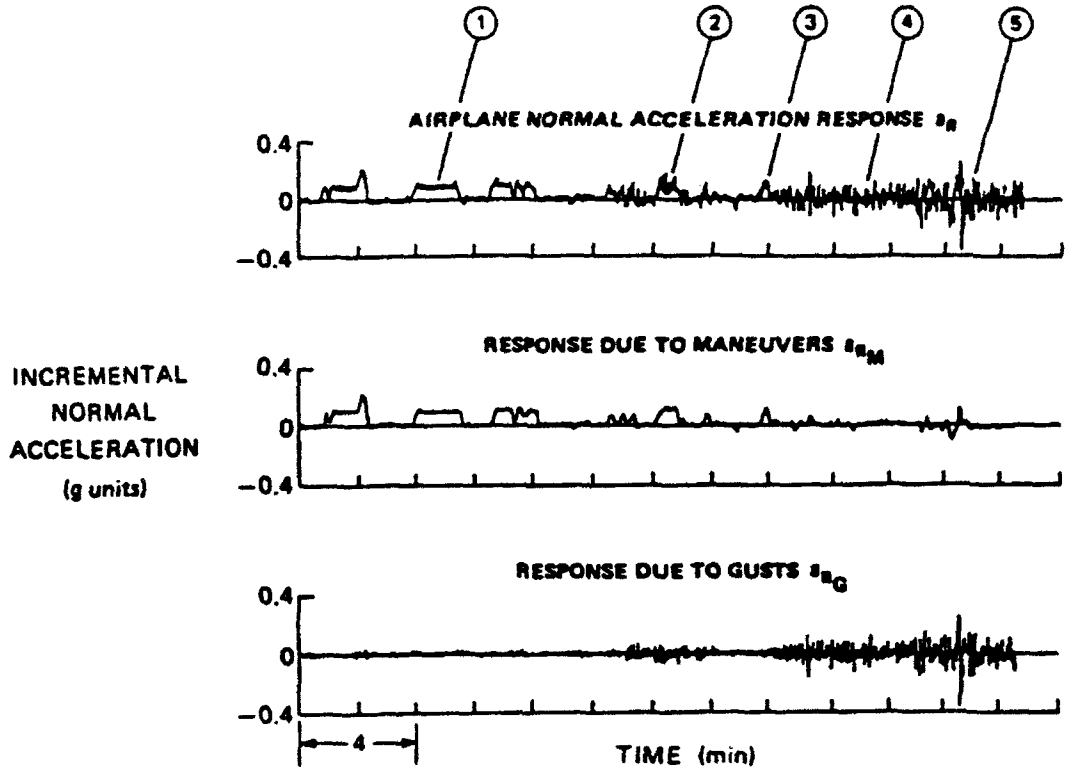

FIGURE 1. FILTER SEPARATION OF NORMAL ACCELERATION TIME HISTORY

suitable detection procedure. To summarize, the following procedure for separating maneuvers and gusts is proposed:

a. Remove the acceleration due to turning maneuvers by subtracting a correction term $\Delta n_{...} = (1/\cos\Phi - 1)$ from the acceleration value.

b. Remove pitch maneuver-induced accelerations at specific points in flight transition such as takeoff/initial climb, climb/cruise, and approach/touchdown.

c. Do not remove the pitch maneuver-induced loads in turbulence, as they are part of the aircraft system response to turbulence.

It will be clear when reevaluating existing data that the above procedures cannot or can only in part be applied because of the required information, e.g., the bank angle is not available. The only advice to be given then is to correct as accurately as possible. It should be realized that in any case, medium-range transport aircraft turbulence is a much more important loading source than maneuvers and that the correction for maneuvers is not of vital importance for obtaining valuable statistical data on gust loads.

3. PEAK/VALLEY SELECTION.

Recall that the objective is to obtain gust statistical data from recorded acceleration traces by reducing acceleration peak/valley values to derived gust velocities. The first step necessary in the procedure is the selection of the peaks and valleys to be reduced. Figure 2 illustrates the procedure generally applied for peak/valley recognition in a continuous load trace to avoid the inclusion of peaks/valleys associated with irrelevant small load variations; a range filter (R) is maintained so that recognized successive peaks and valleys differ at least R in value.
If we wish to reduce recognized acceleration peaks to upward gusts and acceleration valleys to downward gusts, the described peak/valley selection procedure is inadequate. As shown in figure 2, acceleration valleys may still have a positive sign, and an acceleration peak may be negative!
For this reason the analysis of the NACA VGH data, a more drastic peak/valley criterion was used. This is shown in figure 3 and usually indicated as the Peak between Means method. Between two successive crossings of the mean (in case of vertical acceleration the 1.0g -level) only one peak or one valley is recognized. To further ignore irrelevant load variations around 1.0g a threshold zone of $\Delta n = \pm 0.02$ was used in the VGH data reduction, as shown in figure 4 (reference 3).

The amount of peaks/valleys that are rejected by the Peak-between-Means criterion depends on the so-called "irregularity" of the signal. The irregularity factor (k) of a signal is defined as the total number of peaks divided by the total number of crossings of the mean in the positive direction. Figure 5a shows a signal with a relatively high irregularity, while Figure 5b depicts a typical narrow band signal having a very low irregularity. For signals with an irregularity factor equal to 1, the Peak-between-Means criterion does not reject any intermediate peaks or valleys, simply because they are not present in the signal.

The aircraft response to turbulence has a narrow-band band character around the pitch response frequency. Figure 6 presents a part of a c.g. acceleration trace recorded in a Boeing 747 flying through turbulence (reference 4), showing the narrow-band character and associated low irregularity of the signal. Note that application of the Peak-between-Means criterion would lead to recognition of all

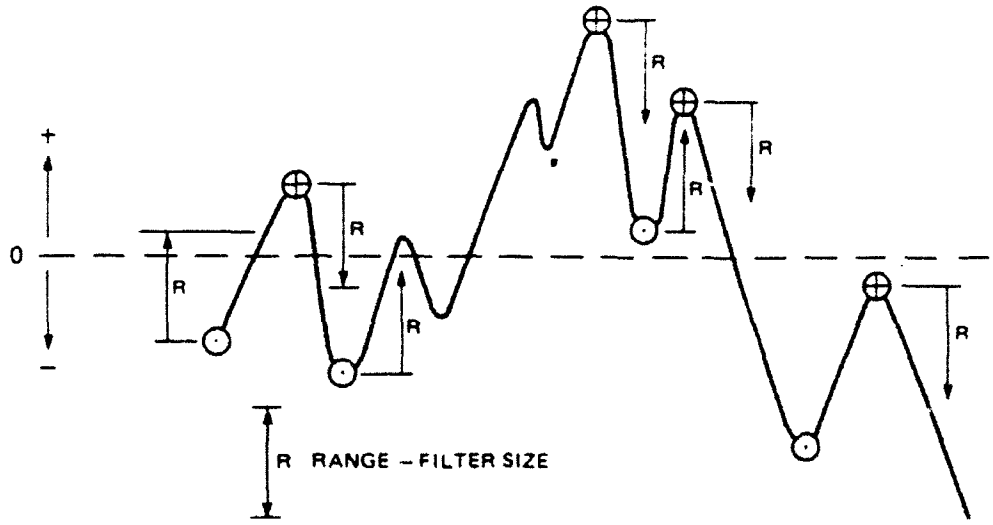

FIGURE 2. CLASSIFICATION OF PEAKS AND TROUGHS USING A RANGE FILTER R

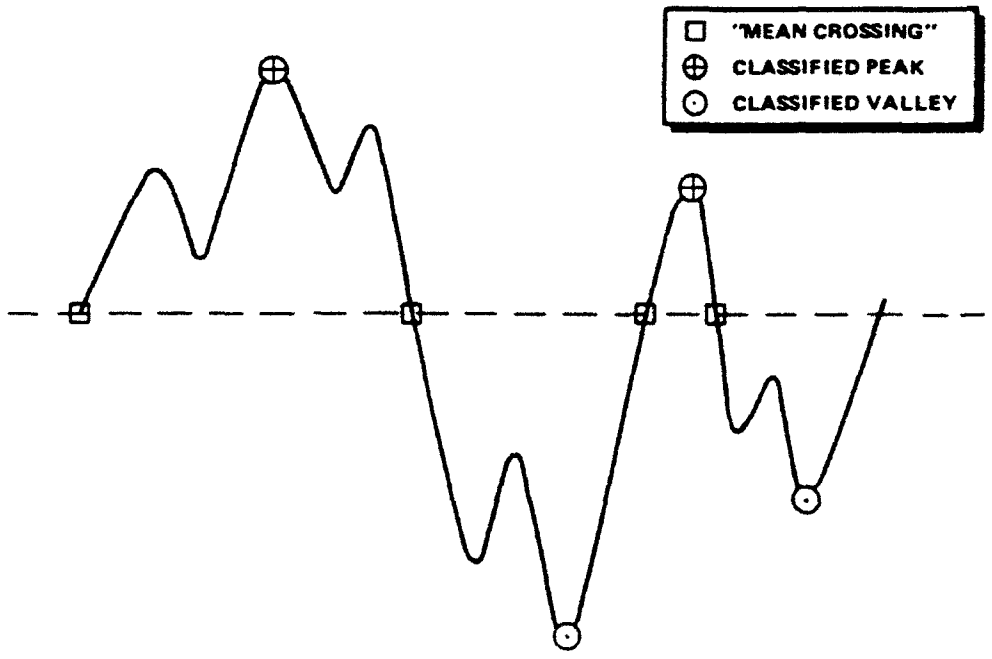

FIGURE 3. PEAK-BETWEEN-MEANS CLASSIFICATION CRITERION

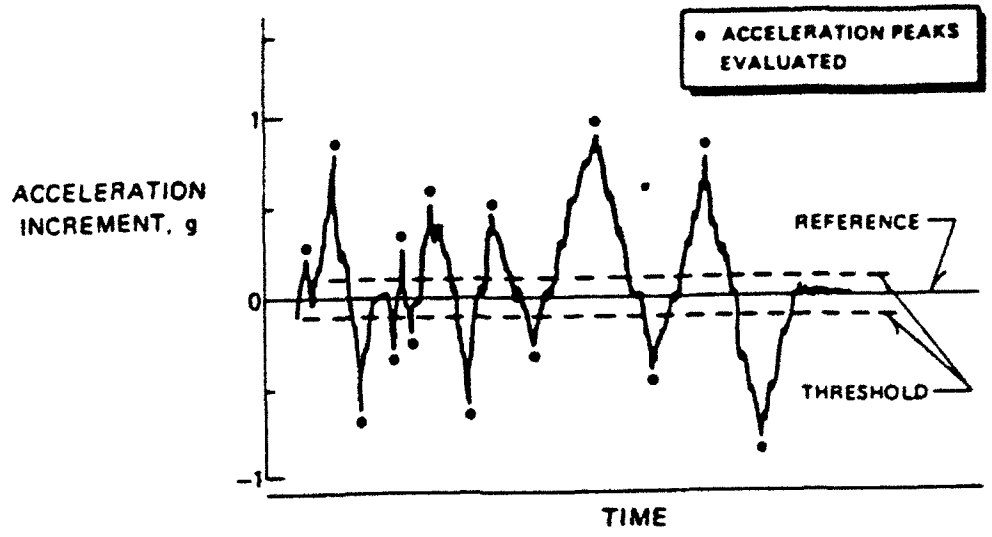

FIGURE 4. METHOD OF EVALUATING ACCELERATIONS FROM VGH RECORDS, BY THE PEAK-BETWEEN-MEANS CRITERION (FROM REFERENCE 3)

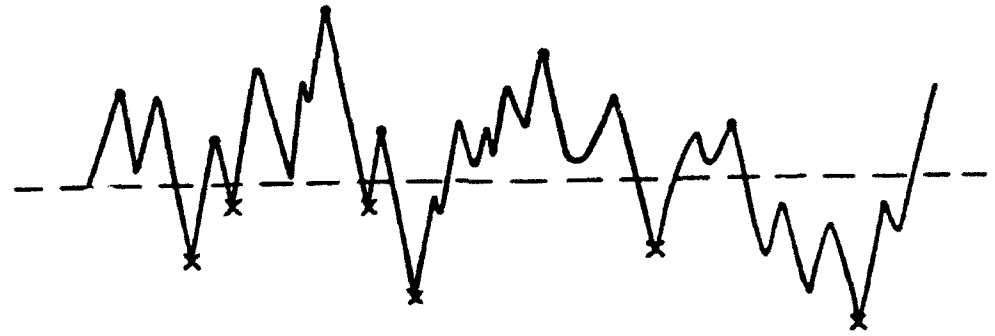

a) BROAD-BAND SIGNAL, IRREGULARITY k>>1

• RECOGNIZED PEAK
× RECOGNIZED VALLEY

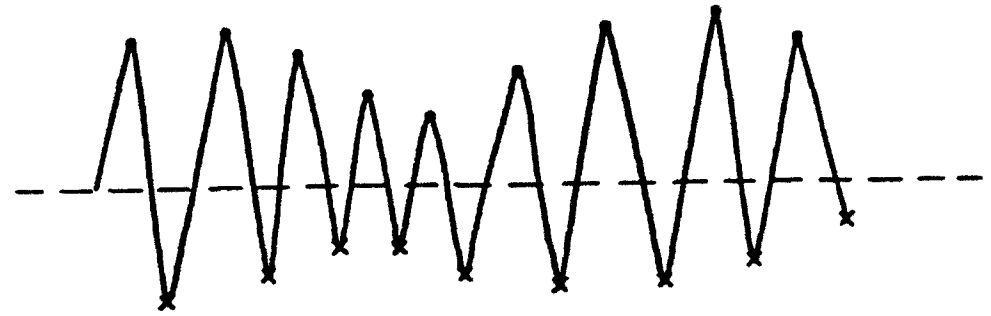

b) NARROW BAND SIGNAL, IRREGULARITY ≈ 1

FIGURE 5. EFFECT OF SIGNAL CHARACTER ON PEAK/VALLEY REDUCTION BY PEAK-BETWEEN-MEANS CRITERION

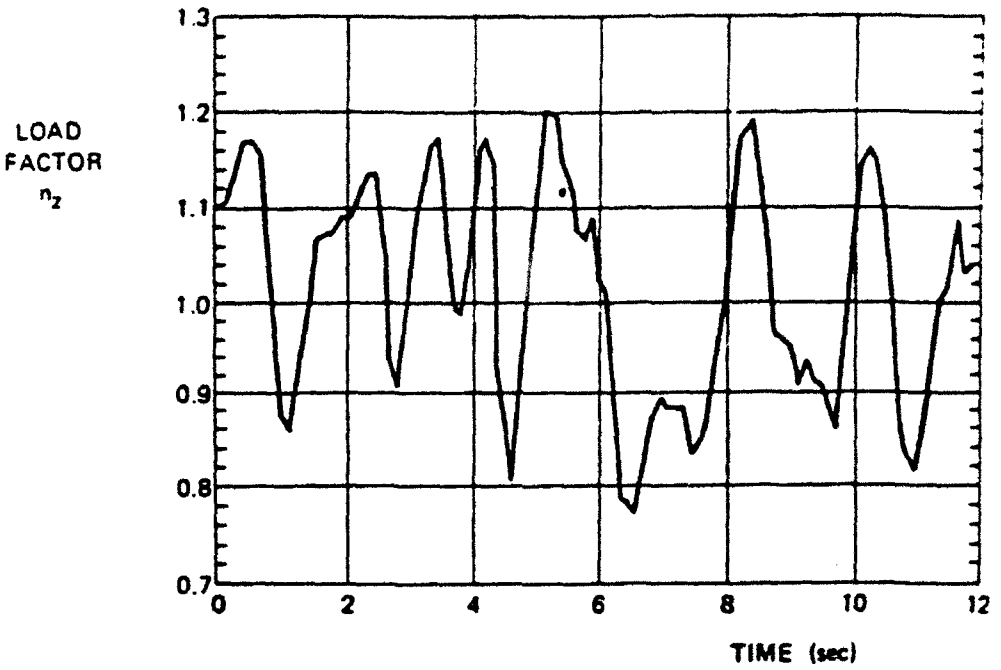

FIGURE 6. EXAMPLE OF RECORDED ACCELERATION TRACE (B747 IN TURBULENCE)

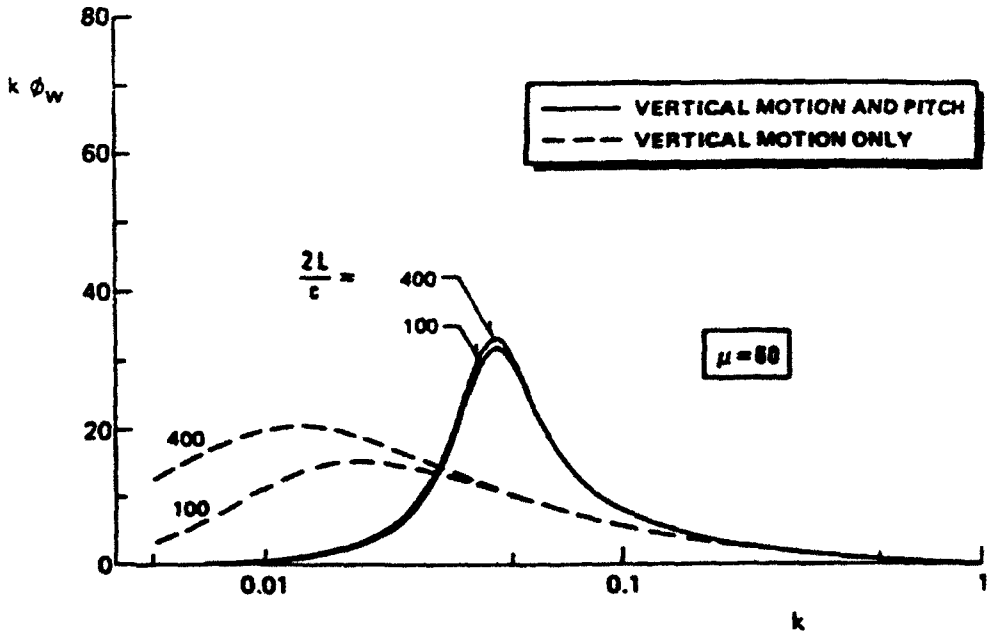

FIGURE 7. DISTRIBUTION OF RESPONSE FOR ONE AND TWO DEGREES OF FREEDOM (FROM REFERENCE 8)

the main turning points in the load sequence. Hence, the Peak-between-Means criterion is less drastic than may appear at first glance when applied to aircraft acceleration data. The Peak-between-Means criterion is well suited to be applied in the analysis of gust-induced accelerations. Also in order to remain compatible with the existing NACA VGH gust data base, it is proposed to use this criterion in the reanalysis of existing data sources as well as in future data acquisition projects.

4. REDUCTION OF Δn_z-PEAKS/VALLEYS TO GUST VELOCITIES.

Two methods for the reduction of acceleration peaks to derived gust velocities will be defined based on essentially different representations of atmospheric turbulence. The first is based on a discrete-gust concept. The aircraft c.g. response to gust is described by one parameter, indicated as $\bar{C}$. Recorded acceleration peaks are reduced to derived gust velocities U_{de}. The gust statistics that will eventually be obtained describe the number of exceedings per kilometer of U_{de} for a number of altitude bands.
The second method is based on a continuous-gust concept. The aircraft c.g. response to gust is described by two parameters, namely $\bar{A}$ and N(0). The recorded acceleration peaks are reduced to derived gust velocities U_{σ}.
The gust statistics obtained initially will have the form of U_{σ}-exceedance curves for a number of altitude bands. These curves may be further evaluated to yield for the various altitude bands the PSD-gust parameters P_1, P_2, b_1 and b_2.
It is proposed to use both methods simultaneously in the analysis of acceleration peak data. Thus, two sets of gust statistics will be obtained: one based on a classical discrete-gust model and easily comparable with old data and the other set based on a more advanced and realistic gust concept.

4.1. DISCRETE-GUST APPROACH.

The atmospheric turbulence is thought to consist of separate discrete bumps with a specific gust profile and magnitude U. The discrete-gust bump induces an aircraft c.g. acceleration with maximum value Δn_z . This Δn_z is related to U by:

$$\Delta n_z = \bar{C} \cdot U \qquad (4.1)$$

Equation 4.1 can be used in the opposite direction to calculate the magnitude U of the gust that caused a recorded incremental load factor Δn_z:

$$U = \Delta n_z / \bar{C} \qquad (4.2)$$

The response function $\bar{C}$ is generally a function of the shape and length of the gust and the response properties of the aircraft. In NACA Report 1206 (reference 5) the response factor $\bar{C}$ was calculated under the following assumptions:

a. The gust has a (1 - cos) shape with a length of 25-wing chords.

b. The aircraft is assumed to be infinitely stiff and to respond only in plunge (and not in pitch).

c. Aerodynamic inertia is included.

The result found for $\bar{C}$ could be approximated by:

$$\bar{C} = \frac{\rho_o V_E C_{L_\alpha}}{2\, mg/S} F(\mu_g) \qquad (4.3)$$

where $F(\mu_g)$ is the so-called gust-alleviation factor, reading:

$$\mu_g = \frac{.88\ \mu_g}{5.3 + \mu_g} \qquad (4.4)$$

The above formula is the well-known so-called "Pratt formula", derived in reference 5. It has been used extensively, not only for reducing the NACA VGH data, but also in airworthiness requirements for defining gust design load factors. The physical reality of the Pratt formula is rather weak. The assumption of a gust length that is a function of the size of the aircraft flying is inappropriate, and the assumption of plunge freedom only is very restrictive. The great advantage, however, of the Pratt formula is its simplicity.

For this reason, and in order to maintain compatibility with the existing gust data bases which have been obtained using the Pratt formula, it is proposed to use this formula in the reevaluation of other data sources and in the analysis of new data.

4.2 PSD APPROACH.

4.2.1 Determination of $\bar{A}$.

Rather than a deterministic sequence of discrete bumps, gust activity can be described as a random process of atmospheric turbulence. The c.g. acceleration response of an aircraft flying through a stationary random gust field with rms value σ_w will also be stationary random, with rms value $\sigma_{\Delta n}$. The ratio $\sigma_{\Delta n}/\sigma_w$ is called $\bar{A}$. This ratio $\bar{A}$ is a response factor that is to a large extent equivalent with $\bar{C}$ described in the paragraph 4.1. This equivalence has led to the formulation of a quasi-discrete PSD-gust velocity U_σ, for which holds

$$\Delta n_z = \bar{A} \cdot U_\sigma$$

This formulation has found its way into current airworthiness requirements, where design values for U_σ are defined as a function of altitude (FAR part 25, Appendix G). Full discussion of PSD methods is outside the scope of this report and reference must be made to the appropriate textbooks. At this point, simply recall that $\bar{A}$ is found by integretation over all frequencies of the aircraft transfer function squared times the normalized power spectral density function of turbulence:

$$\bar{A} = \left[\int_o^\infty |H_{\Delta n,w}(j\omega)|^2\, \Phi_w^n(\omega) \cdot d\omega \right]^{\frac{1}{2}} \qquad (4.5)$$

Thus, $\bar{A}$ may be considered as a <u>weighted average response</u>, taking into account the aircraft response characteristics, that is the sensitivity for specific wavelengths (through the transfer function H) on the one hand and the atmospheric properties (which wavelengths do occur?) through the PSD function on the other. The $\bar{A}$ approach is based on a much more realistic turbulence model. Moreover, note that in calculating $\bar{A}$ the real wavelength distributions as occurring in turbulence were considered rather than assuming an aircraft size-dependent gust as done for calculating $\bar{C}$.

$\bar{A}$ may be calculated using the same simplifying assumptions with regard to aircraft response as in the Pratt formula, that is infinite stiffness and response freedom in plunge only. Such calculations have been made in the past, for example in reference 6 and reference 7. However, as pointed out in references 8 and 9, the assumption of no response in pitch is unrealistic here. The weathercock effect associated with pitch response freedom greatly reduces the aircraft response on gusts with long wavelengths. Figure 7 compares the aircraft c.g. acceleration response for an aircraft with plunge freedom only and plunge and pitch. (The value of the discrete-response function $\bar{C}$ is not very dependent on the inclusion of pitch freedom because the assumed gust wavelength of 25 chords is very short). Hence, a simple but realistic expression for $\bar{A}$ should at least consider plunge and pitch response freedom. Houbolt (reference 8) calculated $\bar{A}$ values for a wide variety of aircraft, aircraft conditions, and flight conditions. Somewhat to his surprise he found that the $\bar{A}$ for a wide range of aircraft could be approximated accurately by using the following expression:

$$\bar{A} = \frac{\rho_0 V_E C_{L_\alpha}}{2\, mg/S} \cdot F(PSD) \qquad (4.6)$$

$$\text{where } F(PSD) = \frac{11.8}{\sqrt{\pi}} \left(\frac{\bar{c}}{2L} \right)^{\frac{1}{3}} \sqrt{\frac{\mu_g}{110 + \mu_g}} \qquad (4.7)$$

The discrete-response factor $\bar{C}$ and the continuous-response factor $\bar{A}$ may be compared by using the expression for F(PSD) with $F(\mu_g)$ as given in (4.4):

$$F(\mu_g) = \frac{.88\, \mu_g}{5.3 + \mu_g}$$

Note that in F(PSD) the aircraft response is described by two parameters, namely μ_g and $\bar{c}$. The parameter $\bar{c}$ is used in combination with the turbulence scale L and defines the size of the aircraft in relation to a typical gust wave length. Recall that in the Pratt formula such a parameter is avoided artificially by assuming that the typical wavelength is a constant times the wing chord $\bar{c}$.

Figure 8 depicts $F(\mu_g)$ and F(PSD) as a function of μ_g for some values of $\bar{c}/L$. The expression given above for A, as derived by Houbolt, is as easy to calculate as $\bar{C}$ according to Pratt and has in our opinion a much better physical background, both with regard to the turbulence model and with regard to the aircraft response model. It is proposed to reduce all Δn peaks to U_σ values using the above Houbolt formula.

4.2.2 The N(0) Problem.

4.2.2.1 Review of the problem.

According to the discrete gust concept, the turbulence consist of a discrete number of gusts or bumps per kilometer; each aircraft flying through this turbulence encounters the same number of bumps; each bump U_{de} causes one load bump $\Delta n = \bar{C} \cdot U_{de}$. The exceedance curve per km for a specific altitude/flight condition has the form:

$$N(\Delta n) = B_1 e^{-\frac{\Delta n}{a_1 \bar{c}}} + B_2 e^{-\frac{\Delta n}{a_2 \bar{c}}} \quad .$$

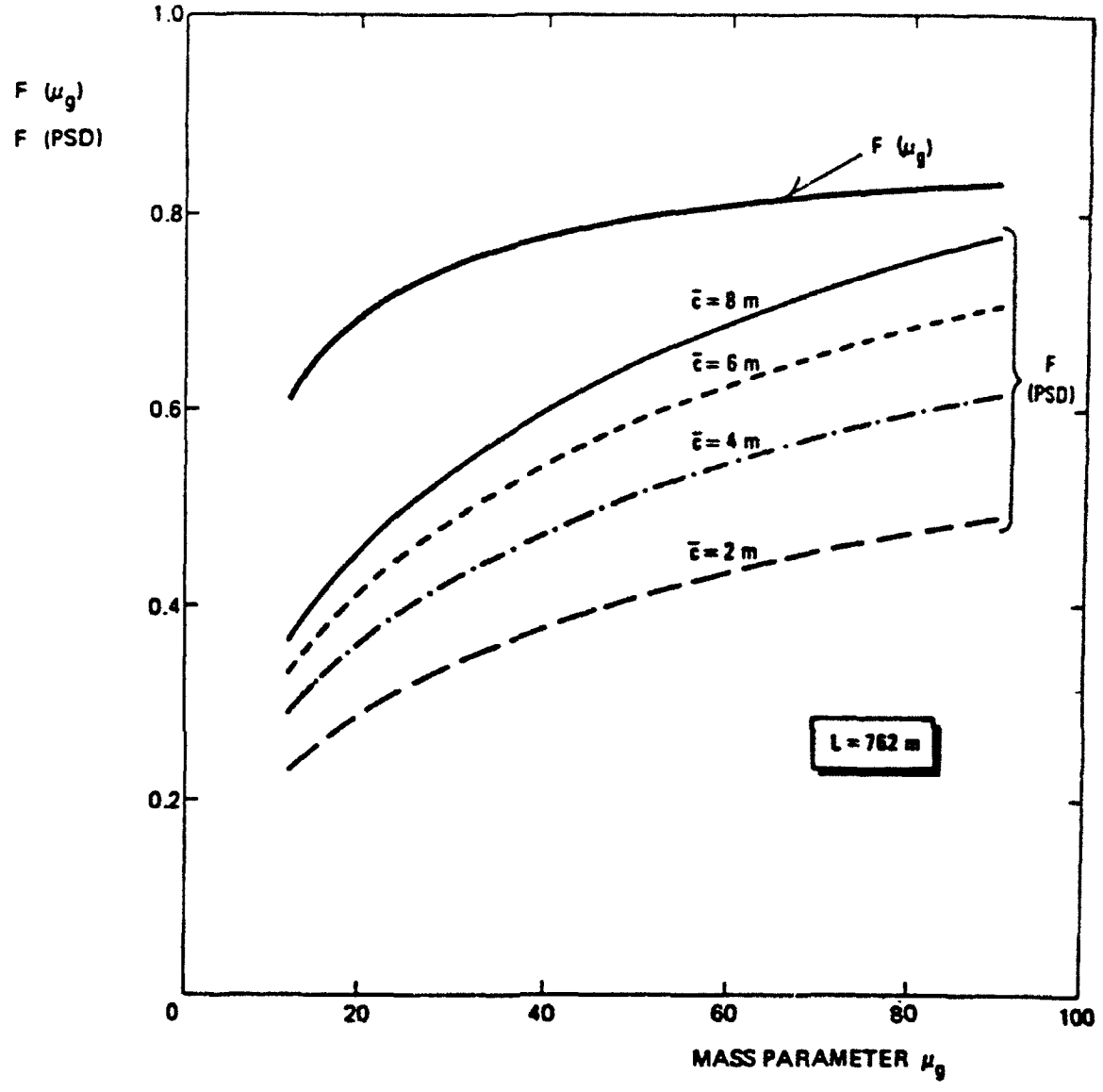

FIGURE 8. THE DISCRETE- AND PSD- BASED GUST ALLEVIATION FACTOR

Note that the total number of Δn bumps per km is equal to B_1+B_2

For the PSD-gust concept, the situation is different. The number of Δn response peaks depends on the aircraft response properties through the parameter N(0). Consequently, the exceedance curve has the form:

$$N(\Delta n) = N(0)\left[P_1 e^{-\frac{\Delta n}{b_1\bar{A}}} + P_2 e^{-\frac{\Delta n}{b_2\bar{A}}}\right]$$

Note that the total number of Δn bumps per km is equal to $N(0)[P_1 + P_2]$, thus this depends on the aircraft response parameter N(0). The questions to be answered are:

a. Should the N(0)-effect be included in the Δn-data reduction procedures?

b. If the answer is yes, how should this be done?

$$N(0) = \frac{496}{\pi\bar{c}}\cdot(\mu_g)^{-.46} \qquad \text{[per km]}$$

$$\text{or } N(0) = N_o(0)\cdot\left(\frac{\rho}{\rho_0}\right)^{.46} \qquad \text{[per km]}$$

$$\text{where } N_o(0) = \frac{496}{\pi\bar{c}}\left[\frac{2m}{S\ \rho o\ C_{L_\alpha}\ \bar{c}}\right]^{.46} \qquad \text{[per km]}$$

To answer the first question, it is necessary to study the possible variations in N(0): if N(0) would be approximately equal for all aircraft types and, e.g., be only a function of altitude, one might ignore the N(0) effect, or rather assume a constant N(0) value, for example in NACA 4332. (reference 6), where for the conversion of discrete-gust data into a PSD model, fixed N(0) values of 6 per km (10 per mile) and 4.7 per km (7.5 per mile) for storm and non-storm turbulence respectively were assumed. To study this N(0) variation, an approximate formula given by Houbolt (reference 8) for N(0) will be used (see Fig. 9):
Table 1 presents calculated $N_o(0)$ values for a wide range of commercial aircraft, for three different weight configurations namely M.TOW, operations weight empty and an average weight. It may be noted that the $N_o(0)$ values cover a wide range, from 20 for the smallest aircraft at low weight to about 4 for the largest aircraft at maximum weight. From this, the variation in N(0) appears to be too large to be ignored. In the following, a method to include N(0) variation in the Δn-data reduction will be outlined.

4.2.2.2 Accounting for N(0) variation.

The following method is proposed to include N(0) variation when reducing Δn- data to U_σ data (PSD-type data). For each altitude h, a reference value $N(0)_{ref}$ is defined:

$$N(0)_{ref} = \left(\frac{\rho}{\rho_0}\right)^{.46}\cdot N_o(0)_{ref}$$

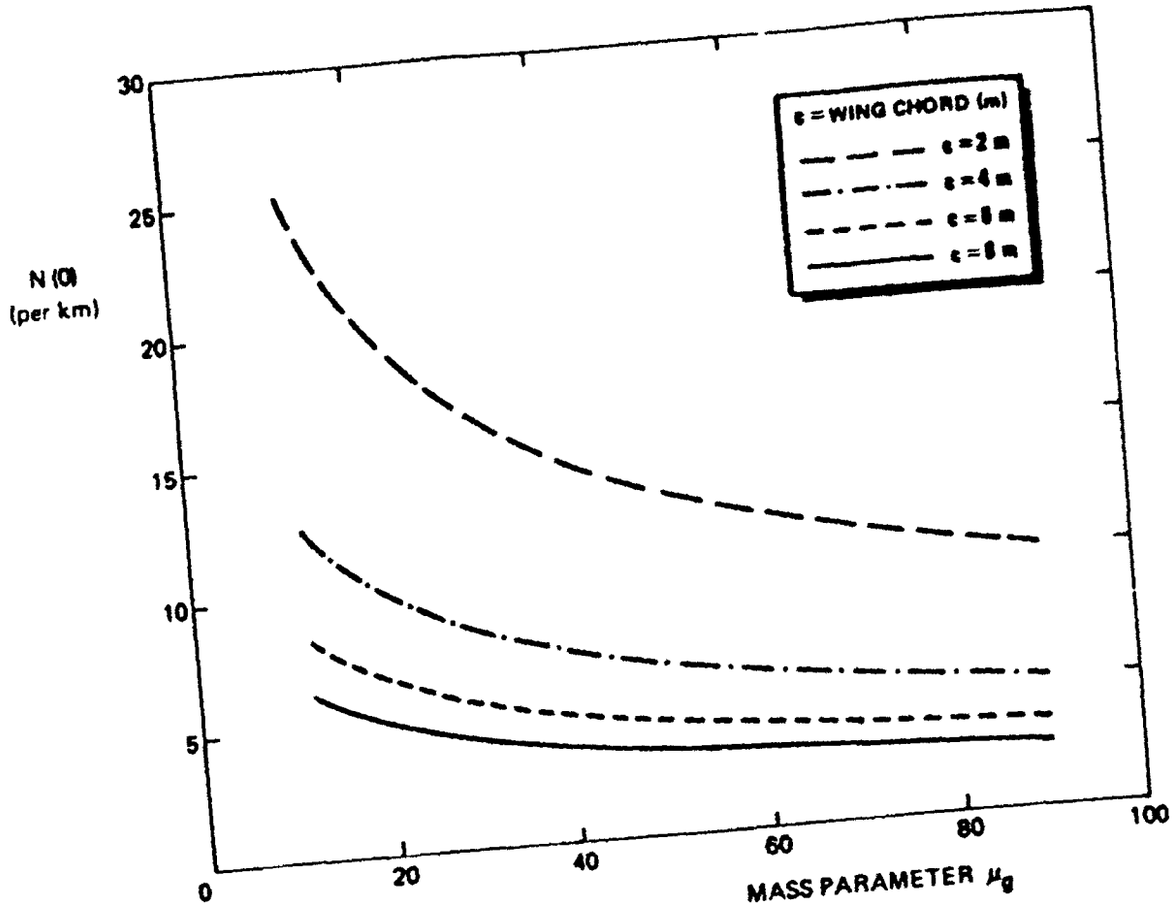

FIGURE 9. N(0) ACCORDING TO HOUBOLT (PSD MODEL, 2-DOF)

where $N_0(0)_{ref}$ is a fixed value and ρ is the density pertaining to the altitude h. Based on the data presented in table 1, the value $N_0(0)_{ref} = 8\ km^{-1}$ is proposed (average for long- and medium-haul transport). A recorded acceleration peak Δn is reduced as follows:

a. Using the values of V,h and aircraft mass, m, at the instant of occurrence of Δn, the response parameters $\bar{A}$ and N(0) are calculated using for the calculation of N(0) the previously presented Houbolt-formula.

b. One recorded Δn peak for an aircraft with N(0) is set equivalent to

$$\frac{N(0)_{ref}}{N(0)} \quad \Delta n \text{ - peaks}$$

for an aircraft with $N(0)_{ref}$.

c. The value Δn is reduced to gust velocity using

$$U_\sigma = \Delta n / \bar{A}$$

In summary one recorded Δn occurrence is reduced to

$$\frac{N(0)_{ref}}{N(0)} \text{ occurances of } U_\sigma.$$

In this way, the reduced acceleration data, U_σ, from different aircraft types and different weight conditions can be added. The resulting statistic, pertaining to a specific altitude band, will have the shape:

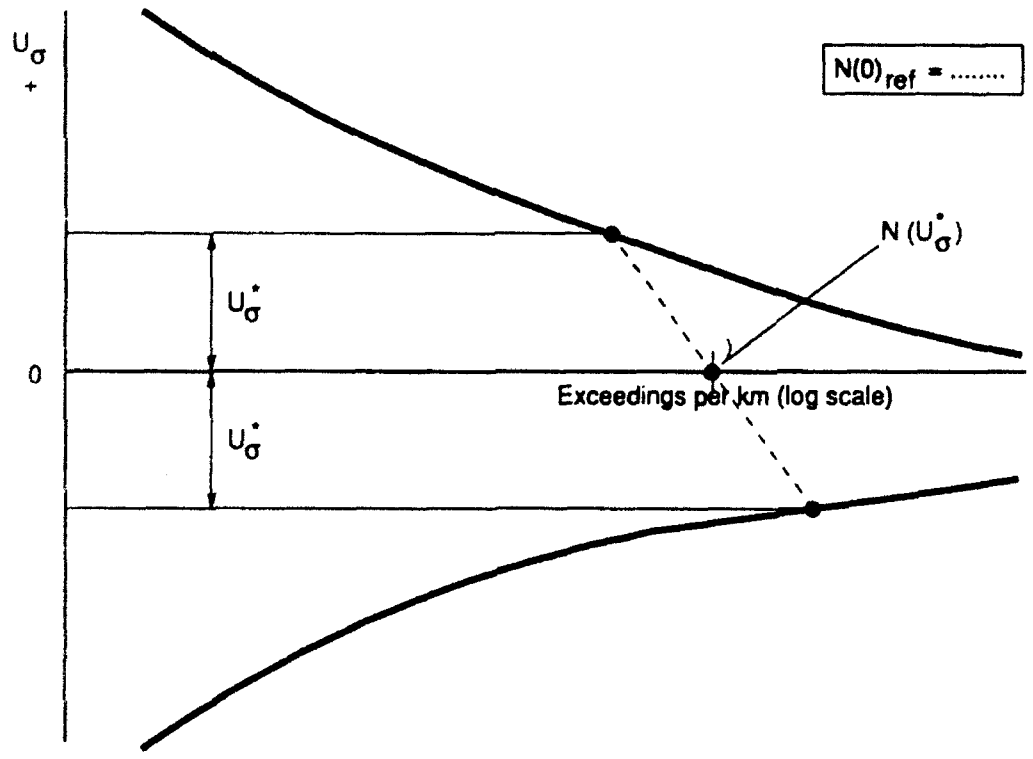

Generally, the number of positive gusts larger than U_σ, $N(U_\sigma^+)$ will be different from the number of negative gusts larger than U_σ, $N(U_\sigma^-)$.

The average number of exceedings of U_σ, $N(U_\sigma)$ is the logarithmic average (see previous figure):

$$N(|U_\sigma|) = \sqrt{N(U_\sigma^+) \cdot N(U_\sigma^-)}$$

The PSD-gust parameters P_1, P_2, b_1 and b_2 can be determined by fitting the curve

$$N^*(U_\sigma) = N(0)_{ref} \cdot \left[P_1 e^{-\frac{U_\sigma}{b_1}} + P_2 e^{-\frac{U_\sigma}{b_2}} \right]$$

to the obtained $N(U_\sigma)$ curve;

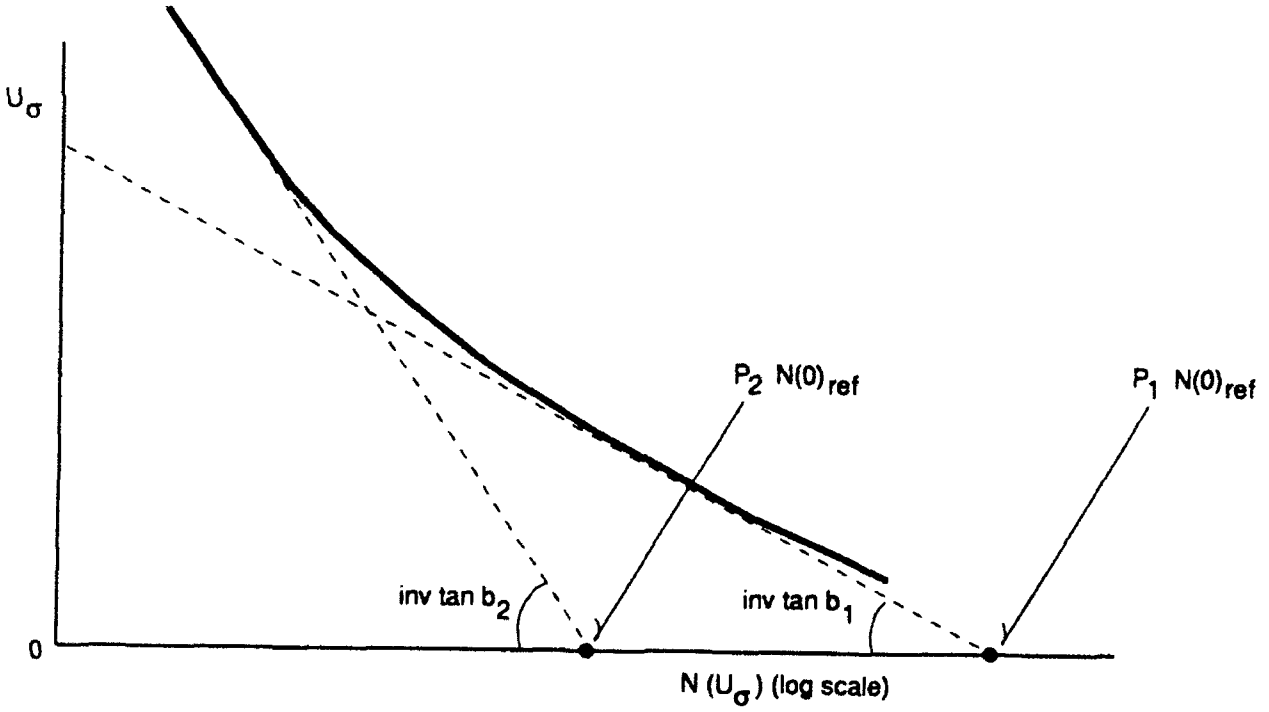

5. CONVENTIONS.

In order to establish a unified procedure for reduction of acceleration data resulting in gust statistics from different sources that can easily be compared, it is desirable to establish firm conventions on a couple of subjects.

5.1 UNIT SYSTEM.

All data must be presented in Standard International(SI) units, with one exception, namely the definition of altitude bands (see section 5.3). The main units pertaining to the SI system are:

time	: second	(s)
length	: meter	(m)
mass	: kilogram	(kg)
force	: Newton	(N)
temperature	: degrees Celsius	(°C)

5.2 VELOCITY DIMENSIONS.

The derived gust velocities U_{de} and U_{σ} are given as equivalent velocities.
As a consequence, the PSD-gust parameters b_1 and b_2 will also be given in terms of equivalent velocities.

5.3 ALTITUDE BANDS.

The derived gust statistics (number of gusts exceeding U_{de}, respectively, U_{σ}, per m or per 1000 m) are presented per altitude band. It is customary in aviation to express flying altitudes in feet rather than meters; the altitude bands will be defined in feet (as an exception, see section 5.1).
The following altitude bands will be used:

<		1500 ft
1500	-	4500 ft
4500	-	9500 ft
9500	-	14500 ft
14500	-	19500 ft
19500	-	24500 ft
24500	-	29500 ft
29500	-	34500 ft
34500	-	39500 ft
>		39500 ft

5.4 TURBULENCE SCALE L.

In accordance with current airworthiness regulations (FAR 25, JAR 25), the turbulence scale L is assumed to be 762 m (2500 ft) at all altitudes.

Note: This convention is usual for U_{de}, but the existing data sources often present U_{σ} and b_1 and b_2 in terms of true velocity

6. REEVALUATION OF EXISTING EUROPEAN LOAD DATA SOURCES.

In the previous paragraphs, a general procedure for reducing c.g. acceleration data to gust load statistics has been established on the assumption that a continuously recorded c.g. acceleration trace were available. To reevaluate existing data sources, this general procedure will be applicable only in part due to the fact that the data has already undergone considerable reduction. In the following, the format of available European Data sources will be reviewed and methods to reduce this data in accordance with our general procedure will be defined.

6.1 NLR BOEING B747 ACMS DATA. (reference 4)

Acceleration peak/valley sequences on a per flight basis are available for 20,205 flights. Successive peaks and valleys have been determined using a range filter size R= 0.18g. The following information is available:

1. Flight profile data: For each flight the speed, altitude, and weight as a function of time have been recorded.

2. Peak data: For each peak or valley, the Δn_z-value, the time at occurrence of the peak, and the flap setting are recorded. For a limited number of flights, the bank angle at peak-occurrence is also recorded.

This implies the following with regard to the applicability of our reduction procedure:

- For only a limited number of flights, the acceleration peak/valley sequence can be corrected for (turning) maneuvers by making the bank angle correction.

- The (corrected) peak/valley sequence may be further reduced using the Peak-between-Means criterion.

- Sufficient data (speed, altitude, weight, 2nd flap setting at time of peak/valley) is available to calculate the response parameters $\bar{C}$, $\bar{A}$, and N(0) associated with each peak/valley so that gust velocities U_{de} and U_{σ} can be derived.

- From the flight profile data the distances flown in the various altitude bands are available to reduce the gust exceedance data for each altitude band to gust exceedings per km

In summary, it appears that the general data reduction procedure is applicable to a very large extent to the B747 ACMS data. It should be kept in mind that, as the B747 ACMS system only recorded acceleration traces when $|\Delta n_z|$ = 0.18g was exceeded (reference 4), the data base is limited to gust velocities higher than those corresponding with this incremental acceleration level of 0.18g.

6.2 ONERA HIGH LOAD DATA.

The ONERA data base contains information about relatively high loads, namely acceleration peaks/valleys larger than $|\Delta n_z|$ = 0.50g, that have occurred in a very large number of flights (about 800,000). These peaks/valleys have been derived from ACMS-recorded acceleration traces using the Peak-between-Means selection criterion. The data base includes, for each recognized peak or valley, the following information:

1. Incremental load factor Δn_z.

2. Aircraft type, tail number, and date.

3. At time of peak: mass, speed, altitude, flap position, and C_{L_α}.

The data base also includes the total number of flights and flight hours analyzed for each aircraft. With regard to applicability of the standard reduction procedures we may conclude that sufficient data is available to calculate $\bar{C}$, $\bar{A}$, and N(0) for each peak/valley occurrance and hence, to calculate exceedance curves for the derived gust velocities U_{de} and U_σ. As no specific flight profile data were recorded, estimated average mission profiles must be used to determine the total distances flown in each altitude band in order to reduce the gust exceedance data to exceedings per km. Overall, the ONERA data appear compatible with our standard reduction procedures.
This data will only provide information about severe and hence relatively rare gusts.

6.3 RAE FATIGUE METER DATA. (Reference 11)

These data were obtained from counting accelerometers measuring center of gravity vertical acceleration. The instrument counts the number of times that preset acceleration levels are exceeded. To avoid spurious counts due to small acceleration variations, the exceedance of a level is only counted after the acceleration has dropped below another predetermined, lower level. More details on the counting procedure, in comparison with the Peak-between-Means method, are described in appendix C.

At intervals of a few minutes the counters were photographed together with an altimeter, speed indicator, and clock. The data available cover about 26,000 hours of flying and include a variety of aircraft. The current data base is available on magnetic tape and is obviously the result of considerable data processing, starting from the original information contained on photographic images. Available data are presented in the following format:

a. For each aircraft type, a large number of intervals are distinguished with regard to:

- Flight segment (e.g., climb, cruise, or descent)
- Altitude (a set of altitude bands is defined)
- Speed (a number of speed ranges are defined)
- Weight (a number of weight ranges are defined)

b. For each interval (one flight segment, altitude band, speed, and weight range), the following information is presented:

- The total time spent and distance flown within the interval.
- The total number of crossings of the various acceleration counting levels.

In order to make these data compatible with the standard reduction procedure, the counted level crossings should be converted to counted peaks and valleys. As shown in appendix C, the difference in number of crossings of two successive (positive) levels is equal to the number of peaks with magnitude larger than the lower and smaller of the higher of these two levels. In appendix B discrete equivalent peak values for all peaks between two level cross counting levels have been defined. Using these values, the counted level crossings for each interval can now be converted to counted peaks/valleys for each interval.

Information (speed, altitude, and weight) is available to calculate $\bar{C}$, $\bar{A}$, and N(0) and hence, to reduce the acceleration peaks/valleys to derived gust velocities U_{de} and U_{σ}. The speed, weight, and altitude are only known within a relatively wide range; hence, the relative accuracy of the derived gust velocities will be lower than for the previously described NLR and ONERA data. In addition, accelerations due to maneuvers cannot be eliminated and that, as explained in appendix C, the applied counting technique may lead to a slight overestimation of relevant peaks.

In summary, we may conclude that the Fatiguemeter data can be reduced and presented such that it is compatible with the other data sources.

7. SUMMARY OF PROPOSED REDUCTION PROCEDURES.

A summary is presented of the successive steps in the general procedure to reduce a recorded acceleration trace to gust velocity data.

7.1 Starting point.

We start with a continuous record of vertical acceleration at or near the aircraft center of gravity. It is assumed that the signal is adequately filtered to eliminate structural responses. If the signal is available in digital form, the signal should in any case be free of frequency components higher than half the sampling rate.

7.2 Elimination of maneuver loads.

If the bank angle history is available, the acceleration history should be corrected for turning maneuver-induced load factor increments by subtraction of a correction term: $\Delta n_{z_{turn}} = (1/\cos\phi - 1)$. If specific pitch maneuvers can be recognized in the signal (e.g., rotation at takeoff, end of climb, etc.) the induced load factor increments should be removed from the acceleration trace.

7.3 Peak/valley selection.

The corrected (i.e., maneuver removed) acceleration history is searched for peaks and valleys using the Peak-between-Means selection criterion.

7.4 Reduction of accelerations to gust velocities.

The classified acceleration peaks and valleys Δn_z are reduced to derived gust velocities, following a discrete-gust approach and a PSD-gust approach respectively.

7.4.1 Discrete Gust.

Each single Δn_z is reduced to one gust U_{de} according to:

$$U_{de} = \frac{\Delta n_z}{\bar{C}} \tag{7.1}$$

$$\text{with : } \bar{C} = \frac{\rho_o V_E C_{L_\alpha}}{2\, mg/S} \cdot F(\mu_g) \tag{7.2}$$

where $F(\mu_g) = \frac{.88\mu_g}{5.3 + \mu_g}$ (7.3)

7.4.2. PSD Gust.

single Δn_z is reduced to $\frac{N_o(0)\,ref}{N_o(0)}$ /gusts /with /magnitude /U_σ , according to:

$$U_\sigma = \frac{\Delta n_z}{\bar{A}} \tag{7.4}$$

$$\text{with } \bar{A} = \frac{\rho_o V_E C_{L_\alpha}}{2\ mg/S} \cdot F(PSD) \tag{7.5}$$

$$\text{where } F(PSD) = \frac{11.8}{\sqrt{\pi}} \left(\frac{\bar{c}}{2L} \right)^{\frac{1}{6}} \sqrt{\frac{\mu_g}{110 + \mu_g}} \tag{7.6}$$

$$\text{and } \frac{N_o(0)_{ref}}{N_o(0)} = \frac{\pi\bar{c}}{62} \left[\frac{2m}{S\rho_o C_{L_\alpha} \bar{c}} \right]^{0.46} \tag{7.7}$$

7.5 GUST EXCEEDANCE CURVES.

The following procedure applies to both U_{de} and U_σ data, but will be described here for U_{de} data only.

7.5.1 Altitude Bands.

The gust peaks/valleys are sorted according to the altitude band in which they occur. The altitude bands have been defined in chapter 5.3.
In addition, the total distance flown within each altitude band is determined.

7.5.2 Gust Exceedance Data.

For each altitude band peak/valley,data areacumulated, resulting in:

- For a set of positive U_{de} values: - number of gust peaks larger than that value
- For negative U_{de} values: - number of "gust valleys" lower than that value

Results are presented as total numbers and, after dividing by the distance flown within the altitude band, as number per kilometer.

7.6 PSD-GUST PARAMETERS.

Determine the average number of exceedings (up or down) of U_σ from

$$N(|U_\sigma|) = \sqrt{N(\dot{U}_\sigma^+) \cdot N(\dot{U}_\sigma^-)}$$

Determine for each altitude band the parameters P_1, P_2, b_1, and b_2 by fitting the curve

$$N^+(U_\sigma) = N(0)_{ref} \left[P_1 e^{-\frac{U_e}{b_1}} + P_2 e^{-\frac{U_e}{b_2}} \right]$$

to the derived $N(|U_\sigma|)$ curve.

$$\text{Here, } N(0)_{ref} = 8 \times \left(\frac{\rho}{\rho_o} \right)^{.46} \quad km^{-1}$$

where ρ is the air density pertaining to the midvalue h_{mid} of the altitude band under consideration.

7.7 REEVALUATION OF EXISTING GUST LOAD DATA SOURCES.

When reevaluating existing gust load data sources, it is important to make these data, as much as possible, compatible with those obtained using the above reduction procedures. Key elements are Peak-between-Means(peak/valley recognition) and
expressions used for $\bar{C}$, $\bar{A}$ and N(0).

The counting accelerometer data are yield level cross data. These should first be reduced to equivalent peak/valley data using the principles outlined in appendix B.

8. CONCLUSIONS.

- A general procedure has been defined for the reduction of measured c.g. accelerations to derived gust velocities.
- Accelerations due to turning maneuvers may be eliminated if the bank angle has been recorded. In addition, the accelerations due to specific pitch maneuvers can be eliminated if they can be recognized in the flight trace.
- If the acceleration data are reduced on the basis of a continuous-gust concept, the variations of the response parameter N(0) should be included. A method to do so has been defined.
- Available European gust data sources can be reevaluated and reduced into a format compatible with the defined analysis procedures.

9. REFERENCES.

1. Crabill, Norman L., The NASA Digital VGH Program- Exploration of methods and final results, NASA Contractor Report 181909, Vol.I: Development of methods
2. Jonge, J.B. de, Assessment of Service Load Experience. 12th Plantema Memorial Lecture, presented at the 15th ICAF Symposium, Jerusalem, June 1989, EMAS Ltd., ISBN 0 947817 35 2
3. Coleman, Thomas L., Trends in repeated loads on Aircraft, NASA TN D-4586, 1965
4. Jonge, J.B. de, Wekken, A.J.P. v.d., Noback, R., Acquisition of Gust Statistics from AIDS-recorded data, in AGARD Report No. 734, december 1987, ISBN 92-835-0426-7
5. Pratt, Kermitt G., Walker, Walter G., A revised gust-load formula and a re-evaluation of V-G data taken on civil transport airplanes from 1933 to 1950, NACA Report 1206, 1954
6. Press, Harry, Steiner, Roy, An approach to the problem of estimating severe and repeated gust loads for missile operations, NACA TN 4332, 1958
7. Hoblit, Frederic M., ed al, Development of a power-spectral gust design procedure for civil aircraft, Technical Report FAA-ADS-53, 1966
8. Houbolt, John C., Status review of atmospheric turbulence and aircraft response, in AGARD Report No. 734, december 1987, ISBN 92-835-0426-7
9. Coupry, Gabriel, Improved reduction of gust loads data for gust intensity, in: AGARDograph 317: Manual on the Flight of Flexible Aircraft in Turbulence, 1991, ISBN 92-835-0617-0
10. Coupry, Gabriel, Progress in the analysis of atmospheric turbulence (in French), in: AGARD Report No.738: Aircraft Response to Turbulence, June 1986, ISBN 92-835-0393-7
11. Kaynes, Ian W., A Summary of the Analysis of Gust Loads Recorded by Counting Accelerometers on Seventeen Types of Aircraft, AGARD Report No.605, December 1972
12. Jonge, J. Ben de, The Analysis of Load -Time Histories by means of Counting Methods, In AGARDograph No.292, "Helicopter Fatigue Design Guide", 1983, ISBN 92-835-0341-4

APPENDIX A
DEFINITION OF C.G. VERTICAL ACCELERATION

The equations of motion of an aircraft may be expressed with reference to an aircraft fixed stability axis system (x,y,z). The origin of this axis system is the aircraft center of gravity and the x axis is defined in such a way that at time t=o the x axis coincides with the direction of the aircraft velocity.

In case of symmetric motion, the equations of motion of an elastic aircraft can be described as follows:

$$m(\dot{w}-U.q) = Z \tag{A.1}$$

$$Iy.\dot{q} = L \tag{A.2}$$

where U = velocity of c.g. in x direction
w = velocity of c.g. in z direction
q = rotational velocity around y axis
m = aircraft mass
Iy = moment of inertia around y axis

and:

$$M_{ii}\ddot{\xi}i(t) + K_{ii}\xi i(t) = Q_i \quad (i=3,..,m) \tag{A.3}$$

with M_{ii} = generalized mass i^{th} mode
K_{ii} = generalized stiffness i^{th} mode
$\xi_i(t)$ = generalized displacement i^{th} mode
Q_i = generalized force i^{th} mode

Equations (A.1) and (A.2) describe the motion of the aircraft center of gravity. The (m-2) equations (A.3) describe the deformation of the structure under loading with respect to the aircraft axis system, (x,y,z). The displacement function of the i^{th} elastic mode reads

$$\vec{W}_i(x,y,z,t) = \vec{\Phi}_i(x,y,z)\xi_i(t)$$

where $\vec{\Phi}_i$ is a vector with components Φ_{xi}, Φ_{yi} and Φ_{zi} in x,y and z direction respectively. The displacement of a point (x^1,y^1,z^1) in the structure in z direction at time t, $W_z(x^1,y^1,z^1,t)$ is equal to

$$W_z(x^1,y^1,z^1,t) = \sum_{i=3}^{m} \Phi_{zi}(x^1,y^1,z^1)\xi_i(t) \tag{A.4}$$

The <u>c.g. vertical acceleration</u> a_z is defined equation A.1

$$a_z = \dot{w} - U.q \tag{A.5}$$

This is the quantity we would like to measure with an on board accelerometer. Unfortunately, the onboard accelerometer is fixed to the (deforming) structure and does not remain in the c.g., which is in fact a virtual point; the acceleration actually measured by the accelerometer mounted in point x=0, y=0,

z=0, is equal to

$$a_z^* = \dot{w} - U\cdot q + \sum_{1}^{m} \Phi_{z1}\,(x=y=z=0)\,\ddot{\xi}_1(t) \qquad (A.6)$$

Figure A-1 presents calculated weighted power spectra $\omega\Phi_{\Delta n_z}(\omega)$ for a short-haul jet transport flying through stationary turbulence. The spectra refer to the real c.g. vertical load factor increment $\Delta n_z = a_z/g$ and the measured value $\Delta n_z = a_z^*/g$

The spectra for Δn_z have been calculated for three cases, namely:

1. The aircraft responds only in plunge (1 DOF)

2. The aircraft responds in pitch and plunge, but is assumed to be infinitely stiff (2 DOF)

3. As in 2, but the aircraft flexibility is taken into account by 8 flexible modes (10 DOF)

We note that inclusion of flexibility has a certain but limited effect on the Δn_z response: the response peak shifts slightly to the left (frequency), and the overall response[1] is slightly lower. Note also that the response is largely restricted to say 18 rad/s or 3 Hz; the energy contained in higher frequencies is negligibly small. Looking now at the spectrum pertaining to the measured load factor increment Δn_Z^*, we note that the spectrum starts to deviate from that of Δn_z above that frequency. The Δn_Z^*-spectrum contains peaks at high frequencies, corresponding with structural response frequencies.

In order to obtain the correct Δn_z signal, the "measured" Δn_Z^* signal must be filtered so that the high-frequency components, above 3 Hz, are eliminated.

The sample frequency of 8 Hz often used in recording c.g. vertical accelerations in transport aircraft is reasonably compatible with this cut-off frequency of 3 Hz. (Sample frequency must be at least two times the highest frequency present, to avoid fold-over effects.)

---

[1] Note: We may recall that the overall Δn_Z response $\sigma_{\Delta n}^2$ is proportional to the area under the curve drawn:

$$\sigma_{\Delta n}^2 = \int_0^\infty \Phi_{\Delta n}(\omega)\,d\omega = \int_{\omega=0}^{\infty} \omega\Phi_{\Delta n}(\omega)\,d(\log\omega)$$

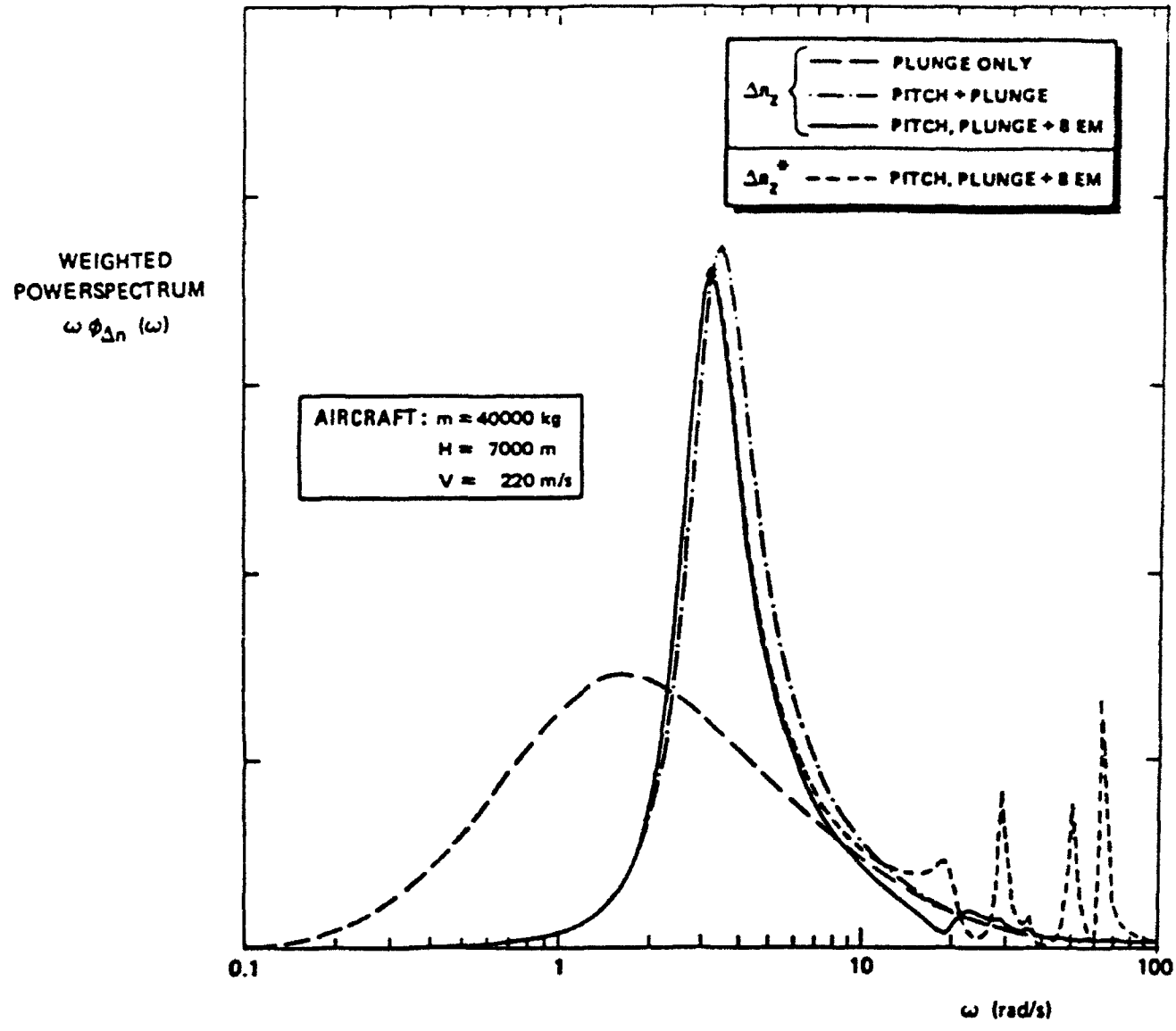

FIGURE A1. WEIGHTED POWERSPECTRUM OF DUE TO TURBULENCE FOR TWIN-ENGINED SHORT HAUL TRANSPORT AIRCRAFT

APPENDIX B
REPLACEMENT OF A LEVEL CROSSING BY AN EQUIVALENT PEAK VALUE

A counting accelerometer presents the number of times that specific acceleration levels Δn_i are exceeded. Suppose that the number of exceedings of level Δn_i is one higher than the number of exceedings of the next higher counting level $\Delta n_{i+1} = \Delta n_i + d\Delta n$. This implies that one peak with magnitude between Δn_{i+1} and $\Delta n_i + d\Delta n$ has occurred. In the following a discrete-equivalent value for the positions of this peak will be derived.

The exceedance curve for Δn, over a limited Δn range, can be fairly well approximated by a straight line in a semi-logarithmic grid.

$$N(\Delta n) = ce^{-S.\Delta n} \qquad (B.1)$$

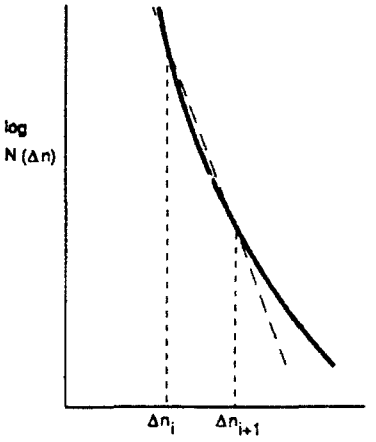

The total number of peaks between Δn_i and $\Delta n_{i+1} = \Delta n_i + d\Delta n$, is equal to

$$N(\Delta n_i) - N(\Delta n_{i+1}) = N(\Delta n_i)\left[1 - e^{-S.d\Delta n}\right] \quad . \qquad (B.2)$$

The probability that a peak within this interval is smaller than $\Delta n_i + d\Delta n^*$ is given by:

$$P(d\Delta n^*) = \frac{1 - e^{S.d\Delta n^*}}{1 - e^{-S.d\Delta n}} \qquad 0<\Delta n^*<\Delta n \qquad (B.3)$$

We will derive equivalent peak values $\Delta n_i + d\Delta n_e$ on the basis of two different criteria:

1. The mean or most probable peak value; $d\Delta n_e = E[d\Delta n^*]$
2. $d\Delta n_e$ is the "median" value $d\Delta n$, that means $P(d\Delta n_e) = \frac{1}{2}$.

Ad 1:

Rewriting (B.3) with $B = S.\Delta n$ and $x = \frac{\Delta n^*}{\Delta n}$ yields.

$$P(x) = \frac{1 - e^{-Bx}}{1 - e^{-B}} \qquad 0<x<1 \qquad (B.4)$$

$$p(x) = \frac{dP}{dx} = \frac{Be^{-Bx}}{1 - e^{-B}}, \qquad 0 \le x \le 1$$

$$= 0 \qquad , \quad x<o \text{ and } x>1$$

$$\mu(x)\ E[x] = \int_{-\infty}^{\infty} p(x) \cdot x \cdot dx = \int_{0}^{1} \frac{B e^{-Bx} x}{(1 - e^{-B})}\ dx =$$

$$\frac{\left[1 - e^{-B}(1 + B)\right]}{B(1 - e^{-B})} \qquad (B.5)$$

Ad 2:

$$1 - e^{-B\bar{x}} = \frac{1}{2}\left[1 - e^{-B}\right]$$

$$e^{-B\bar{x}} = \frac{1}{2}\left[1 + e^{-B}\right]$$

$$\bar{x} = \frac{-1}{B} \ln \frac{1}{2}\left[1 + e^{-B}\right] \qquad (B.6)$$

Numerical values:

The mean $\mu(x)$ and median $\bar{x}$ according to (B.5) and (B.6) respectively are a function of B: $B = S.d\Delta n$ depends on the slope S of the Δn exceedance curve and the difference $d\Delta n$ between successive counting levels. A review of recorded acceleration data, presented in references 4, 10 and 11 revealed that the value of S ranges from about 6 for a steep Δn spectrum to about 15 for a flat spectrum. For example, figure B-1 shows recorded acceleration spectra for the F-28 aircraft, yielding an average S value of about 8.8.

The distance between successive counting levels used in the RAE fatiguemeters (Reference section 1.2) is either $d\Delta n = 0.1$ or $d\Delta n = 0.2$. Thus, the total range for B values is from $0.1 * 6 = 0.6$ to $0.2 \times 15 = 3.0$. Table B-1 gives values for the mean $\mu(x)$ (e.g., B.5) and the median $\bar{x}$ (e.g., B.6) as a function of B. For all B values, the difference between mean and median is relatively small. Over the B range considered, the mean decreases from 0.458 to 0.28 and the median from 0.438 to 0.21. On the basis of these findings, it has been decided to assume average equivalent x values of 0.40 and 0.33 for $\Delta n = 0.10$ and $\Delta n = 0.20$ respectively.

Table B-2 presents the resulting equivalent peak values associated with the crossing levels for the two types of fatigue meters used in the RAE measurements of reference 11.

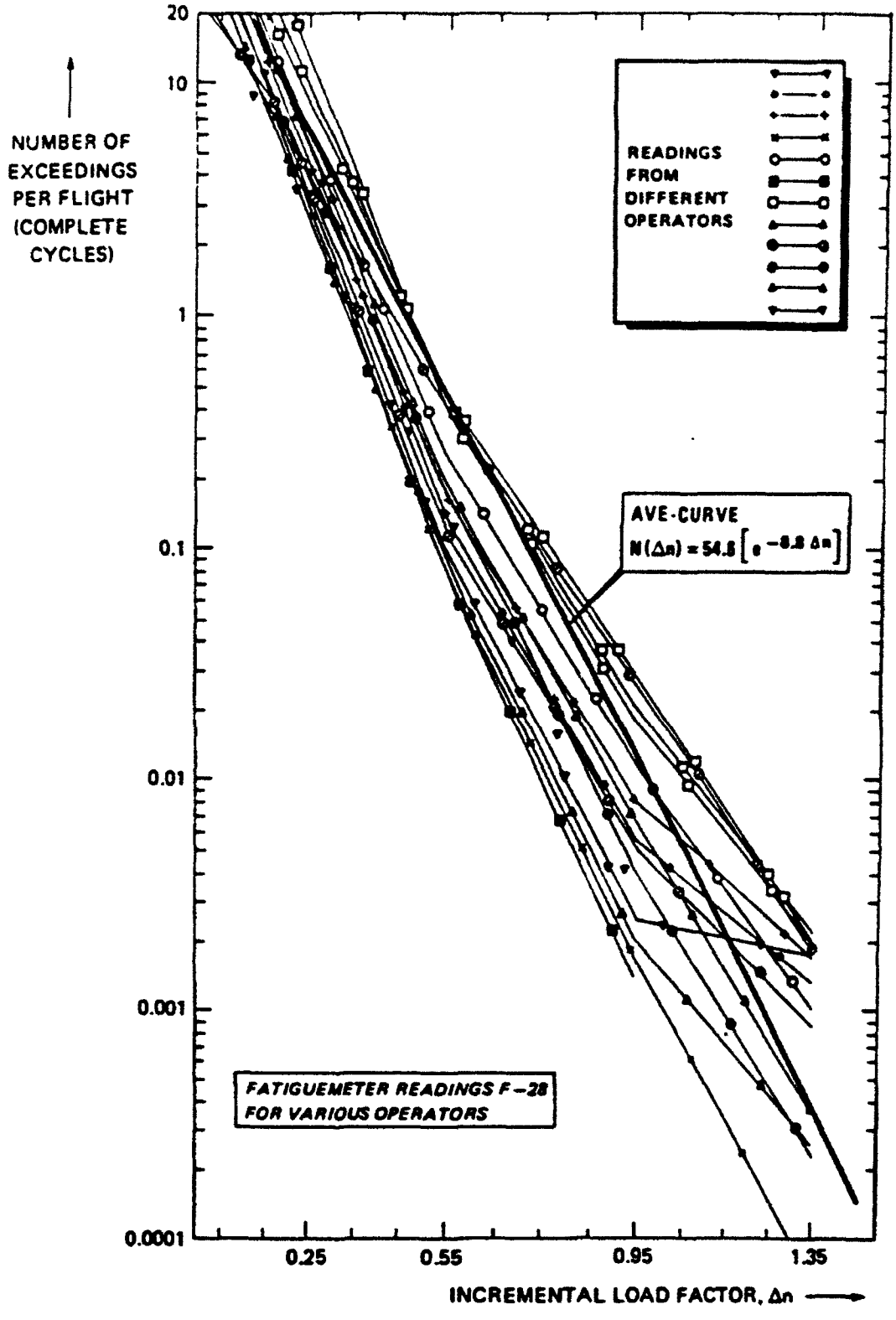

FIGURE B1. EXAMPLE OF RECORDED ACCELERATION SPECTRA

TABLE B-1

MEAN $\mu(x)$ AND MEDIAN $\tilde{x}$ AS A FUNCTION OF B = S*dΔn

B	mean	median
0.5	0.45851	0.43814
0.6	0.45030	0.42610
0.7	0.44214	0.41423
0.8	0.43403	0.40256
0.9	0.42599	0.39110
1.0	0.41802	0.37989
1.1	0.41013	0.36892
1.2	0.40232	0.35822
1.3	0.39460	0.34780
1.4	0.38697	0.33766
1.5	0.37945	0.32782
1.6	0.37203	0.31828
1.7	0.36472	0.30904
1.8	0.35752	0.30009
1.9	0.35044	0.29145
2.0	0.34348	0.28311
2.1	0.33665	0.27506
2.2	0.32994	0.26730
2.3	0.32335	0.25983
2.4	0.31690	0.25263
2.5	0.31057	0.24570
2.6	0.30438	0.23904
2.7	0.29832	0.23263
2.8	0.29240	0.22647
2.9	0.28660	0.22055
3.0	0.28094	0.21485

TABLE B-2

EQUIVALENT PEAK LEVELS TO BE USED IN THE REEVALUATION

OF RAE FATIGUEMETER DATA

MECHANICAL INSTRUMENTS		ELECTRICAL INSTRUMENTS	
cross level* Δn	equivalent peak $(\Delta n + d\bar{\Delta n})$	cross level* Δn	equivalent peak $(\Delta n + d\bar{\Delta n})$
0.23	0.27	0.20	0.24
0.33	0.37	0.30	0.34
0.43	0.47	0.40	0.466
0.52	0.56	0.60	0.666
0.62	0.66	0.80	0.866
0.72	0.76	1.00	1.066
0.82	0.86	1.20	1.266
0.92	0.96	1.40	1.466
1.02	1.10 (1)	1.60	1.68 (1)

Notes: *: from reference 11, table 1

(1): more or less arbitrarily chosen

APPENDIX C
THE COUNTING PRINCIPLE OF THE FATIGUEMETER

Peak count methods and level cross count methods are closely related. The difference in number of crossings of two successive levels is equal to the number of peaks minus the number of valleys between these two levels (reference 12). If the signal in question has a narrow-band character, as in the case of e.g. accelerations due to turbulence, the number of valleys between two positive levels and the number of peaks between two negative levels will approach zero, and the difference in crossings of the two levels will be equal to the number of peaks if the two levels are positive and equal to the number of valleys if the two levels are negative. Figure C-1 illustrates the counting principle of the fatigue meter. A counting level is cocked when the signal crosses that level. The counting of that level crossing is completed when the signal passes another reset level, which is closer to 1g. This counting principle is documented in the literature as restricted level cross counting. If the reset levels for <u>all</u> counting levels were set at 1g ($\Delta n = 0$), the Peak-between-Mean result could be directly obtained from the counted level crossings: the number of peaks between level j and level j+1 would be equal to the difference in crossings of the two levels, even if the signal does not exhibit a narrow-band character.

Table C-1, from reference 11, shows that the reset levels maintained do not fully comply with this criterion. This means that more peaks and valleys might be recognized than according to the Peak-between-Means criterion. From the example of figure C-1, two crossings of level j+1 and one of level j+2 are counted, to be interpreted as one peak above level j+2 and one between j+1 and j+2. The Peak- between-Means criterion would only recognize the one peak above level j+2 and ignore the one between j+1 and j+2. Since the acceleration signal is of narrow band nature and the reset levels for the most relevant counting levels are very near the mean($\Delta n = 0$), it is felt that this effect may be ignored and that differences in counted crossings of successive positive levels may be interpreted as number of peaks between these levels (and valleys in case of successive negative levels.)

TABLE C-1

ACCELERATION INCREMENT LEVELS (G) COUNTED BY THE RAE FATIGUE METERS(ELECTRICAL INSTRUMENTS)

COUNTER COCKED	COUNT COMPLETED
0.2	0.0
0.3	0.0
0.4	0.1
0.6	0.2
0.8	0.3
1.0	0.4
1.2	0.6
1.4	0.8
1.6	1.0

from reference 11

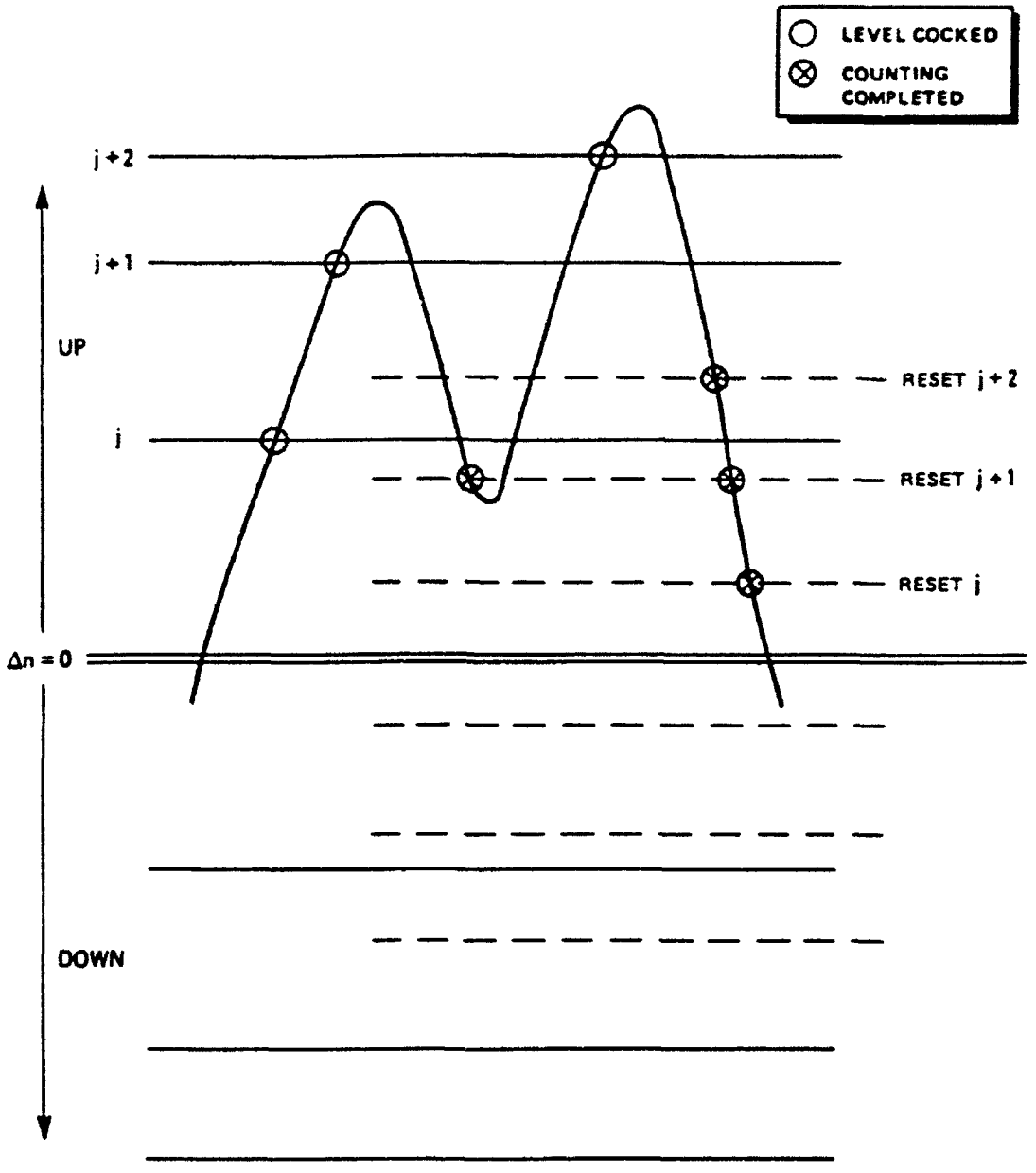

FIGURE C1. COUNTING PRINCIPLE OF THE FATIGUEMETER

TABLE C- 2

VALUES OF UG AND N(0) FOR VARIOUS AIRCRAFT

Altitude = 0 ft rho = 1.225 kg/m^3

Aircraft		S [m^2]	b [m]	Ar [-]	c [m]	Cla* [-/rad]	Maximum Take-off weight MTOW [kg]	μg_o	$N_o(0)$	Max m/S [kg/m^2]	Operational Weight Empty OWE [kg]	μg_o	$N_o(0)$	Average Weight ½(MTOW+OWE) [kg]	μg_o	$N_o(0)$
B747-200	long	511	59.64	7.0	8.57	5.36	377840	26.29	4.10	739	169961	11.82	5.92	273901	19.06	4.75
DC-10(30)	medium	367.7	50.4	6.9	7.30	5.35	263085	29.92	4.53	715	121198	13.79	6.47	192142	21.85	5.24
MD-11	medium/long	338.9	51.66	7.9	6.56	5.50	273289	36.47	4.60	806	125783	16.79	6.58	199536	26.63	5.32
A340-300	long	361.6	58.65	9.5	6.17	5.70	251000	32.25	5.18	694	125500	16.12	7.13	188250	24.19	5.91
B767-300	medium	283.3	47.57	8.0	5.96	5.52	156489	27.44	5.78	552	83461	14.64	7.71	119975	21.04	6.53
A300-600	medium	260	44.84	7.7	5.80	5.48	165000	32.59	5.48	635	86662	17.12	7.37	125831	24.86	6.21
A310-300	medium	219	43.89	8.8	4.99	5.62	157000	41.73	5.69	717	69957	18.59	8.25	113479	30.16	6.60
B757-200 lr	medium	185.25	38.05	7.8	4.87	5.49	113395	37.36	6.13	612	57180	18.84	8.40	85288	28.10	6.99
B757-200 mr	short	185.25	38.05	7.8	4.87	5.49	104325	34.37	6.37	563	57180	18.84	8.40	80753	26.61	7.17
L100-30	medium/long	162.12	40.41	10.1	4.01	5.76	70310	30.66	8.15	434	35260	15.37	11.20	52785	23.02	9.30
B737-300	short	105.4	28.88	7.9	3.65	5.51	62822	48.41	7.26	596	31479	24.26	9.98	47151	36.33	8.29
A320-200	short/medium	122.4	33.91	9.4	3.61	5.69	73500	47.74	7.39	600	39777	25.84	9.80	56639	36.79	8.33
Fokker 100/	Tashort/medium	93.5	28.08	8.4	3.33	5.58	44450	41.79	8.52	475	24540	23.07	11.19	34495	32.43	9.57
Fokker 100	short/medium	93.5	28.08	8.4	3.33	5.58	43090	40.52	8.64	461	24360	22.90	11.23	33725	31.71	9.67
ATP	regional	78.3	30.63	12.0	2.56	5.91	22930	31.63	12.61	293	14238	19.64	15.70	18584	25.64	13.89
Fokker 50	regional	70	29	12.0	2.41	5.92	20820	34.01	12.92	297	12742	20.81	16.19	16781	27.41	14.26
CN-235	regional	59.1	25.81	11.3	2.29	5.86	14400	29.65	14.50	244	9400	19.35	17.65	11900	24.50	15.83
ATR 72	regional	61	27.05	12.0	2.26	5.91	19990	40.12	12.81	328	12200	24.48	16.08	16095	32.30	14.16
Citation S/II	reg./corp.	31.83	15.9	7.9	2.00	5.51	6849	31.84	16.05	215	3655	16.99	21.43	5252	24.41	18.14
SAAB 340	regional	41.81	21.44	11.0	1.95	5.84	12927	44.34	14.15	309	7899	27.09	17.75	10413	35.72	15.63
King Air C90A	corp.	27.31	15.32	8.6	1.78	5.60	4581	27.45	19.30	168	2985	17.88	23.50	3783	22.67	21.08
Metro III	commuter	28.71	17.37	10.5	1.65	5.80	6577	39.04	17.70	229	4268	25.33	21.60	5423	32.18	19.35
Jetstream	reg./corp.	25.2	15.85	10.0	1.59	5.75	7350	52.12	16.11	292	4415	31.30	20.37	5883	41.71	17.85

Note: Approximated by $C_{l_\alpha} = 1.15 \frac{6Ar}{Ar+2}$